ISIJ International, Vol. 41 (2001), Supplement, pp. S52-S55

Instability Phenomena at Bath Surface Induced by Top Lance Gas Injection

Takehiko KUMAGAI[1)] and Manabu IGUCHI[1)]

[1)]Division of Materials Science and Engineering, Graduate School of Engineering, Hokkaido University, North 13, West 8, Kita-ku, Sapporo, 060-8628 Japan.

Top lance gas injection processes are extensively used in metallurgical engineering. When the exit of the top lance is placed near the bath surface, a downward bubbling jet is generated in the bath. The flow patterns of the downward bubbling jet are classified into seven categories mainly with gas flow rate. Instability phenomena of the bubbling jet appear when the gas flow rate is higher than a certain critical value. The phenomena are strongly dependent on the penetration depth of the bubbling jet into the bath, and hence, an empirical relation is proposed for the penetration depth as a function of the gas flow rate, nozzle diameter and vessel diameter.

KEY WORDS: Refining process; gas injection; top lance; swirl motion; Froude number.

1. Introduction

Injecting gas downward into a bath from a top lance is effective for dissolving the gas into liquid in the bath as well as mixing the bath[1-4]. The gas interacts with the liquid and induces instability phenomena at the gas-liquid interface, especially when the exit of the top lance is placed near the bath surface. Such phenomena are greatly responsible for the performance of the processes. However, little is known about the instability phenomena except for very simple cases. We therefore tried to clarify the relationship between the phenomena and operating conditions such as the bath diameter, nozzle diameter and the distance from the initial bath surface to the nozzle exit, referred to as nozzle height.

2. Experimental apparatus and procedure

A schematic diagram of the experimental apparatus is shown in **Fig. 1**. The cylindrical vessel is made of transparent acrylic resin. The liquid phase in the bath was deionized water, and the gas phase was air.

The diameters of the acrylic vessels were 120mm, 200mm and 400mm, and the corresponding vessel heights were 340mm, 340mm and 600mm. Three types of lances were prepared for introducing air into the water in the vessel. The inner nozzle diameters were 1.0mm, 2.0mm and 4.0mm. The center line of each lance was so set that it overlapped the center line of the vessel. The position of the nozzle exit, H_n, was varied from 20mm beneath the initial bath surface to 20mm above it. The air flow rate, Q_g, was changed from 3.6cm^3/s to 840cm^3/s at each injection position using a massflow controller and a regulator.

The behavior of a downward bubbling jet or a bubble dispersion region generated in the bath was strongly dependent on the penetration depth of the jet, H_J. The penetration depth therefore was measured with a high-speed video camera and a still camera. Symbols used in this study are shown in **Fig.2**.

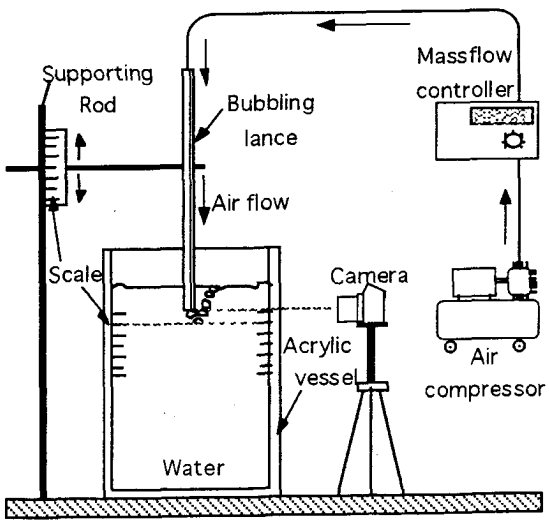

Fig. 1 Experimental apparatus for top lance bubbling

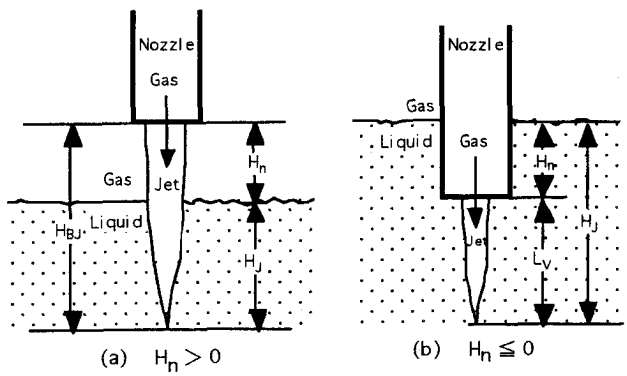

Fig. 2 Definition of H_{BJ}, H_n, H_J and L_V

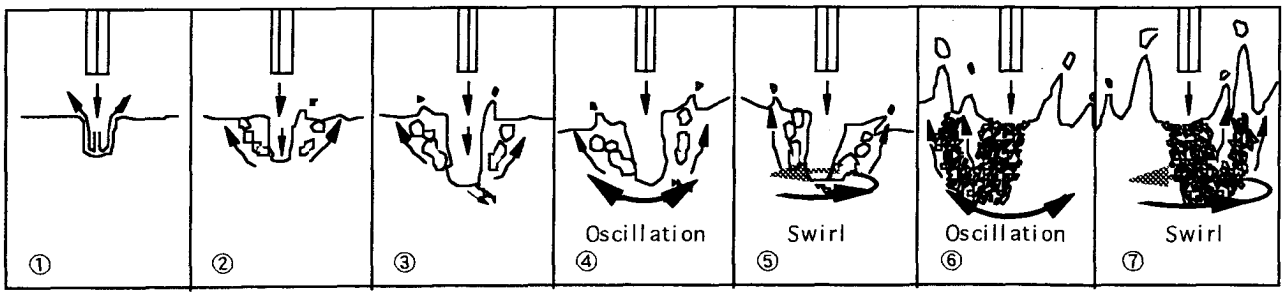

Fig. 3 Classification of surface instability behavior induced by top lance injection

When the nozzle exit is placed above the bath surface ($H_n>0$), H_J is expressed by:

$$H_J = H_{BJ} - H_n \quad (1)$$

where H_{BJ} is the distance from the nozzle exit to the deepest position where bubbles can reach and H_n is the distance from the nozzle exit to the initial bath surface. When the nozzle exit is placed in the bath, H_J is expressed by

$$H_J = H_n + L_V \quad (2)$$

An empirical relation for the penetration length L_V is given elsewhere[5].

$$L_V = 4.1 d_{ni} Fr_m^{1/3} \quad (3)$$

$$Fr_m = \rho_g Q_g^2 / (\rho_L g d_{ni}^5) \quad (4a)$$

$$= (4/\pi)^2 \rho_g v_n^2 / (\rho_L g d_{ni}) \quad (4b)$$

where Fr_m is the modified Froude number representing the ratio of the inertial force to the buoyancy force of injected gas, ρ_g is the density of the gas, Q_g is the gas flow rate, ρ_L is the density of liquid, g is the acceleration due to gravity, and d_{ni} is the inner diameter of the nozzle.

Existing measured values of L_V are known to be approximated by Eq.(3) within a scatter of ±30%, although the evidence is not given here[5,6].

3. Experimental results and discussion

3.1 Classification of instability phenomena of bubbling jet

In a strict sense, the wave motion of liquid is closely related to the pattern of the bubbling jet. The wave motion was, however, found to be strongly dependent on the bath diameter, D, in a very complicated manner. Accordingly, only the motions of bubbling jets will be discussed in this study.

The patterns of bubbling jets generated in the bath using a top lance can be classified into seven categories as shown in **Fig.3**. They are summarized as follows:

(1) A short gas column is formed beneath the nozzle exit. The column is stable and does not disintegrate into bubbles. The vertical cross-section of the bubble column is not always parabolic[7].

(2) A gas column is formed beneath the nozzle exit, just like the pattern (1). Relatively large bubbles are generated near the bottom of the column and they rise beside the column. The column is stable.

(3) In addition to the generation of a bubble column and relatively large bubbles, very small bubbles are generated at the bottom of the column and they penetrated into the bath. The column is stable.

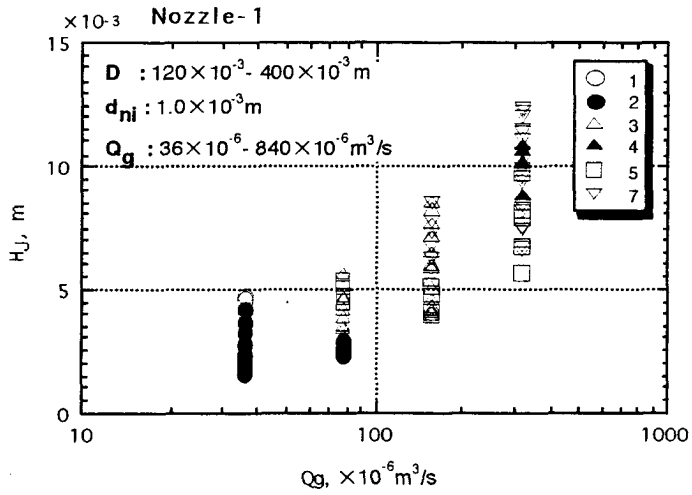

Fig. 4 Existing regions of the patterns 1-7 for $d_{ni} = 1.0\times10^{-3}$ m

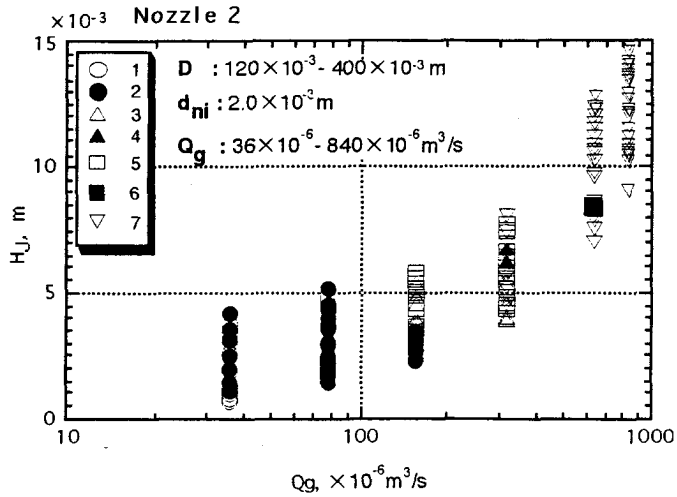

Fig. 5 Existing regions of the patterns 1-7 for $d_{ni} = 2.0\times10^{-3}$ m

(4) The generation of a gas column, relatively large bubbles and very small bubbles is the same as the pattern (3). The gas column, however, oscillates periodically in the radial direction.

(5) The generation of a gas column, relatively large bubbles and very small bubbles is the same as the pattern (3). The gas column swirls around the vessel axis.

(6) A gas column disintegrates into many bubbles with different diameters. The bubbling jet oscillates periodically in the radial direction.

(7) A gas column disintegrates into many bubbles with different diameters. The bubbling jet swirls around the vessel axis.

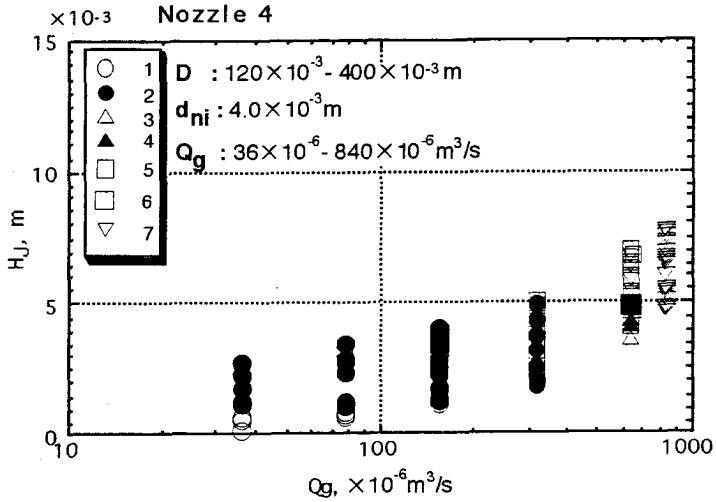

Fig. 6 Existing regions of the patterns 1-7 for $d_{ni} = 4.0 \times 10^{-3}$ m

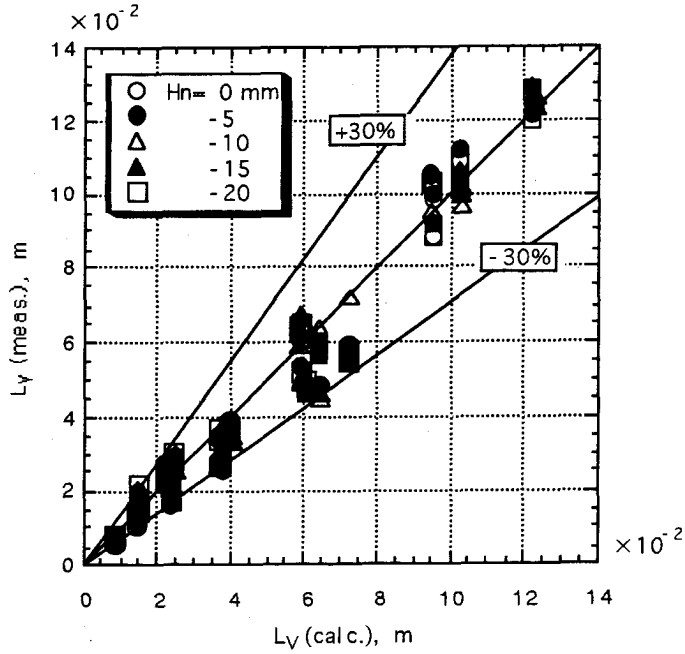

Fig. 7 Comparison of measured with predicted values of L_V

The behavior of bubbling jet classified into the patterns (4) to (7) was caused through the effect of hydrodynamic instability. Under these conditions the bath would be strongly agitated, and, as a result, the mixing time would be significantly shortened. However, this subject is beyond the scope of this study.

Figures 4 through 6 show some examples of the existing regions of the patterns 1 to 7. For each gas flow rate, the symbols at the highest and lowest positions were observed at $H_n = -20$mm and $+20$mm, respectively. Although the data are limited, it is evident that the existing regions of the patterns are dependent on the bath diameter, D, just like the upward gas injection[8-10]. In order to complete the flow pattern map, H_n must be changed over a wide range.

3.2 Estimation of penetration depth of bubbling jet

According to the abovementioned results, the instability phenomena of bubbling jet are closely associated with the penetration depth H_J. When the nozzle exit is immersed in the bath (see Fig.2(b)), it is easy to evaluate H_J because H_J is given by Eq.(2) and L_V can be evaluated from Eq.(3).

Figure 7 demonstrates that the presently measured values of L_V can be predicted by Eq.(3) within a scatter of $\pm 30\%$.

On the other hand, no empirical relation is not given for H_J in the case that the nozzle exit is placed above the bath surface (see Fig.2(a)). In the following, an empirical relation for H_J in Fig.2(a) will be derived. It is assumed that the gas jet impinges on the bath surface at a velocity of v_n', which is lower than the nozzle exit velocity, v_n, as shown in **Fig.8**. According to a previous study[11], v_n' is expressed by

$$v_n' = v_n \quad (H_n/d_{ni} < 1.26) \tag{5a}$$

$$= v_n / \{[0.00523(H_n/d_{ni} - 1.26)^2] + 1\} \quad (1.26 \leqq H_n/d_{ni} < 17.2) \tag{5b}$$

$$= v_n / [0.167\,(H_n/d_{ni}) - 0.543] \quad (17.2 \leqq H_n/d_{ni}) \tag{5c}$$

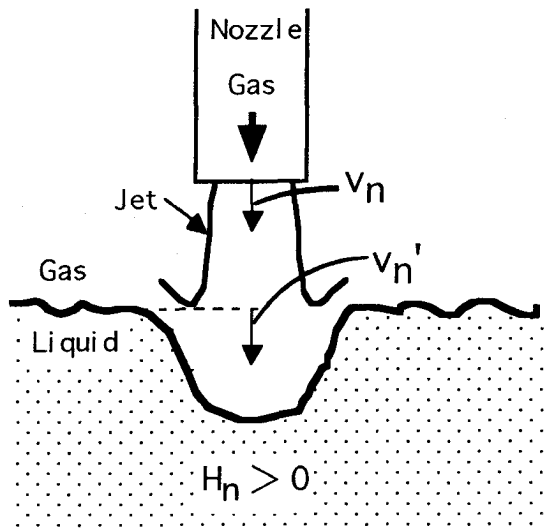

Fig. 8 Schematic of gas jet impinging on bath surface

Figure 9 shows relationship between v_n' and H_n calculated from Eq.(5a) to Eq.(5c). The velocity ratio, v_n'/v_n, decreases drastically in the far field ($H_n/d_{ni} \geqq 1.72$).

We further assume that the penetration depth of gas into the bath, H_J, can be also predicted by Eq.(3) and replace v_n by v_n' in Eq. (4b).

$$H_J=4.1\ d_{ni}\ [Fr_m']^{1/3} \qquad (6)$$

$$Fr_m'=(4/\pi)^2\ \rho_g(v_n')^2/(\rho_L g\ d_{ni}) \qquad (7)$$

where Fr_m' is also the modified Froude number.

Figure 10 compares the measured values of H_J with calculated values from Eq.(6). The measured values can be approximated by Eq.(6) within a scatter of ± 30%. Accordingly, the penetration depth both for the cases shown in Figs.2(a) and 2(b) is predictable with sufficient accuracy.

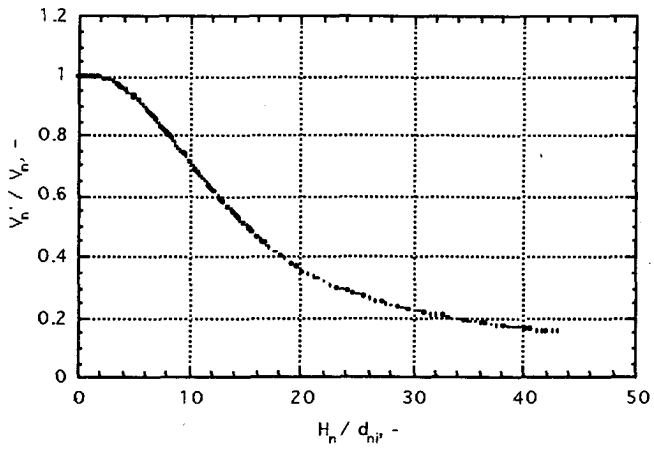

Fig. 9 Relation between v_n' and H_n

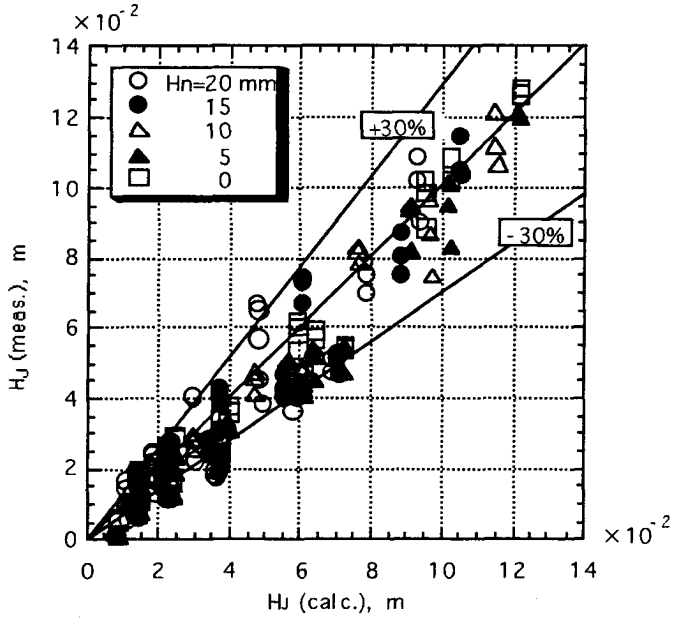

Fig. 10 Relation between measured and predicted values of H_J

4. Conclusions

The patterns of bubbling jets generated by top lance gas injection were classified into 7 categories, as shown in Fig.3. The patterns were found to be significantly related to the penetration depth of the bubbling jet. The instability phenomena appeared when the penetration depth was large. When the nozzle exit was placed above the bath surface, an empirical relation,Eq.(6), was proposed for the penetration depth.

REFERENCES

1) J. Szekey: Fluid Flow Phenomena in Metals Processing, Academic Press, New York, (1979).
2) K. Mori and M. Sano: *Tetsu-to-Hagane'*, **67** (1981), 672.
3) Recent Trend of Steelmaking Technology Utilizing Gas Mixing, ISIJ, Tokyo, (1984).
4) 100th and 101th Nishiyama Memorial Seminar, ISIJ, Tokyo (1984)
5) M.Iguchi, M. Uemura, H. Yamaguchi, T. Kuranaga and Z. Morita: *Tetsu-to-Hagane'*, **80** (1994), 18; *ISIJ Int.*, **34**, (1994), 973
6) B. U. N. Igwe, S. Ramachandran and J. C. Fulton: *Metall. Trans.*, **4** (1973), 1887.
7) I. Muchi, M. Otsuki, and S. Asai: *Tetsu-to-Hagane'*, **53** (1967), 424.
8) M.Iguchi, S. Hosohara, T. Koga, R. Yamaguchi and Z. Morita: *Tetsu-to-Hagane'*, **78** (1992), 1778; *ISIJ Int.*, **33**, (1993), 1037
9) M.Iguchi, S. Hosohara, T. Kondoh, Y. Itoh and Z. Morita: *Tetsu-to-Hagane'*, **79** (1993), 934; *ISIJ Int.*, **34**, (1994), 330
10) M.Iguchi, Y. Itoh and Z. Morita : *Tetsu-to-Hagane'*, **80** (1994), 189.
11) M.Iguchi and E. Yamada: *Trans. Jpn. Soc. Mech. Eng., B*, **55** (1989), 1524.